

MODELLING THE CREEP OF TIMBER BEAMS

Tomi Toratti

Rakenteiden Mekaniikka, Vol. 25
No 1, 1992, ss. 12 - 35

SUMMARY

The calculation method described in ref. Toratti (1991) is used here to model the creep of structural size timber beams in natural outdoor humidity conditions. The constitutive models of wood were determined from test results of small sized specimens. These models are used here in an analysis to determine the creep of a structural size beam. The main principle in the computation is that only a single cross section of the beam is analysed. The analysis is thus two dimensional. In every time step the cross section moisture distribution is computed by the finite difference method using an explicit scheme. The moisture distribution results are then used to calculate the creep cumulated during this time step using a trapezoidal scheme. The axial strain of the cross section is computed iteratively until the internal stresses are in equilibrium with the external loads and the compatibility requirement of linear strain distribution are satisfied. The calculation method is used to model 10 year and 50 year creep behaviour of timber and glulam beams.

MOISTURE TRANSFER - CREEP ANALYSIS

The computation method of the analysis is based on the finite difference method to compute the transient moisture and on the 'method of successive approximations' the stress and strain distributions. These numerical methods have been introduced in early literature (Patankar 1980; Mendelson & Hirschberg & Manson 1959). Both of these numerical methods have been used before in a number of studies. In this study, these two numerical methods are combined. This is particularly important in the study of the long term behaviour of wood, since for wood the deformations under sustained loads have been found to be very sensitive to moisture content changes.

The input required to define the material behaviour in the analysis consists of material parameters involved in moisture transfer as well as parameters involved in the constitutive relations. The input needed for the moisture transfer analysis are the sorption isotherm, diffusion coefficient and surface resistance. The constitutive equations include a moisture content dependent elastic modulus a basic creep model and a mechano-sorptive creep models and a shrinkage coefficient parallel to grain. The problem-dependant inputs are the cross section size, the loading and the relative humidity of the surrounding air as a function of time.

MOISTURE TRANSFER PROPERTIES

The moisture technical parameters used in the finite difference analysis of moisture distribution were determined based on a literature survey (Toratti 1991). The following were used (moisture content of wood [kg/m³] as potential):

$$\begin{aligned} \text{Diffusion coefficient: } D(u) &= 1.0 \times 10^{-10} \exp(2.28 u) \quad [\text{m}^2/\text{s}] \\ \text{Surface emissivity: } S &= 0.5 \times 10^{-7} \quad [\text{m/s}] \\ \text{Sorption isotherm: } u &= 0.01 \text{ RH} / (-0.000928 \text{ RH}^2 + 0.12545 \text{ RH} + 0.33467) \quad [-] \end{aligned} \quad (1)$$

where RH is the relative humidity of air [%]
 u is moisture content [-]

The above relations and parameter values were determined based on a literature survey and on preliminary experiments carried out by the author.

DEFORMATION ANALYSIS AND MATERIAL PROPERTIES

The constitutive model and material parameters introduced in the following have been determined from previous creep tests of clear wood in bending (Toratti 1991; Mohager & Toratti). The constitutive equation of wood is assumed to be linear with respect to stress. The strain of wood when subjected to sustained loading and moisture content variation is assumed to consist of the following additive parts: elastic ϵ_E , normal creep ϵ_{visk} , mechano-sorptive creep ϵ_{ms} and free shrinkage strains ϵ_u , eq.(2)

$$\epsilon(t) = \epsilon_E + \epsilon_{visk} + \epsilon_{ms} + \epsilon_u \quad (2)$$

The deformations are calculated only parallel to grain. A linear strain distribution, Bernoulli hypothesis, over the cross section is assumed:

$$\epsilon(x,y) = \partial v / \partial z - y \partial^2 \omega / \partial z^2 \quad (3)$$

Where: v is displacement in z (grain) direction
 ω is displacement in y direction (height direction)

The strain increment at each node during the current time step is composed of:

$$\Delta \epsilon = \Delta \epsilon_E + \Delta \epsilon_{visk} + \Delta \epsilon_{ms} + \Delta \epsilon_u \quad (4)$$

Where: $\Delta \epsilon_E$ is the elastic strain increment
 $\Delta \epsilon_{visk}$ is the normal creep strain increment
 $\Delta \epsilon_{ms}$ is the mechano-sorptive creep strain increment
 $\Delta \epsilon_u$ is the shrinkage strain increment

Elastic strain increment

The elastic strain depends on the elastic modulus and its dependence on moisture content. The following values were used here:

$$\epsilon_E = \sigma J_0(u) , \quad (5)$$

where $E_0(u) = (J_0(u))^{-1} = 14000(1 - 1.06 u)$ [MPa]
 u : moisture content [-]

The elastic strain increment can be given as:

$$\Delta \epsilon_E = J_0 \Delta \sigma + \Delta J_0 \sigma \quad (6)$$

Where J_0 is the elastic compliance
 ΔJ_0 is the increment of elastic compliance due to the moisture content dependence of the elastic modulus

Normal creep strain increment

The normal creep function is given in a Kelvin series form which consists of six

(n=6) Kelvin elements having retardation times of 0.01, 0.1, 1, 10, 100, 5000 days. Normal creep in the convolution integral form is then as:

$$\epsilon_{visk} = J_0(u_{ref}) \int_0^t \{ \sum J_n (1 - \exp(-(t-t')/\tau_n)) \partial\sigma/\partial t' \} dt' \quad (7)$$

where

$J_1 = 0.0676$ [-]	$\tau_1 = 0.01$ [days]
$J_2 = -0.0018$ [-]	$\tau_2 = 0.1$ [days]
$J_3 = 0.0626$ [-]	$\tau_3 = 1$ [days]
$J_4 = 0.0683$ [-]	$\tau_4 = 10$ [days]
$J_5 = 0.1427$ [-]	$\tau_5 = 100$ [days]
$J_6 = 0.8373$ [-]	$\tau_6 = 5000$ [days]
$u_{ref} = 0.2$ [-]	
σ : stress [MPa]	
t : time [days]	

The strain increment at each time step is then calculated using the trapezoidal rule from (Thelandersson 1987):

$$\Delta\epsilon_{visk} = J_0(u_{ref}) \sum J_n (1 - \exp(-\Delta t/\tau_n)) (\Delta\sigma/2 + \sigma_n^{hist}) \quad (8)$$

Where the n stress history terms, σ_n^{hist} , are updated after each time step:

$$\sigma_n^{hist} = (\sigma_n^{hist} + \Delta\sigma/2) \exp(-\Delta t/\tau_n) + \Delta\sigma/2 \quad (9)$$

Mechano-sorptive creep strain increment

The mechano-sorptive creep limit concept as well as the shrinkage strain model eq.(14) have originally been proposed by Hunt & Shelton (1988). The creep limit model can be formulated in a constant stress as eq.(10) and this defines that mechano-sorptive creep approaches a limit value as moisture increments are introduced.

$$\epsilon_{ms}(t) = J^\infty \{1 - \exp(-c (\sum |\Delta u|))\} \sigma \quad (10)$$

Recent creep test results under long term loading and subjected to many relative humidity cycles (Mohager & Toratti 1991) did not follow the creep limit model. The deformation was found to increase during subsequent humidity cycles without reaching a limit value. The increment of deformation during a humidity cycle was highest during the first cycles and decreased during the

following cycles, but the increment did not show a tendency to vanish. The creep limit model was thus slightly changed to account for this observed behaviour in the following equations.

The mechano-sorptive model and parameter values derived from previous tests are used without altering the material parameters values. It was assumed that for tension stress the creep approaches a limit value and the creep limit model is used. For compression stress the model is a combination of the creep limit and the linear model. This linear part is assumed to be due to losses of stability of the microfibrils under compression resulting in the formation of slip planes. In addition it is assumed that this linear part of the mechano-sorptive strain is irrecoverable as all other mechano-sorptive and normal creep strain is fully recoverable under changing humidity conditions when unloaded.

For tension stress:

$$\epsilon_{ms}(t) = J^{\infty} \int_0^t \left\{ 1 - \exp\left(-c \left(\sum_0^t |\Delta u| - \sum_0^{t'} |\Delta u| \right)\right) \right\} d\sigma(t'), \quad (11)$$

For compression stress:

$$\epsilon_{ms}(t) = J^{\infty} \int_0^t \left\{ 1 - \exp\left(-c \left(\sum_0^t |\Delta u| - \sum_0^{t'} |\Delta u| \right)\right) \right\} d\sigma(t') + J_0(u_{ref}) e \int_0^t \sigma(t') |du(t')|, \quad (12)$$

$$\begin{aligned} \text{where } J^{\infty} &= 0.7 J_0(u_{ref}) \\ c &= 2.5 [-] \\ e &= 0.1 [-] \end{aligned}$$

A trapezoidal rule to integrate the mechano-sorptive deformation is used. The mechano-sorptive creep is incremented at each time step by eq.(13) if the sign of stress is negative. For positive sign stress the last term on eq.(13) is left out. The Boltzmann superposition principle is assumed valid for normal as well as for mechano-sorptive creep, with the provision that the last term in eq.(12) and eq.(13) is irrecoverable.

$$\Delta \epsilon = J^{\infty} (1 - \exp(-c |\Delta u|)) (\Delta \sigma / 2 + \sigma_{hist}) + \sigma J_0(u_{ref}) e |\Delta u|, \quad (13)$$

$$\text{where, } \sigma_{hist} = (\sigma_{hist} + \Delta \sigma / 2) \exp(-c |\Delta u|) + \Delta \sigma / 2, \\ \text{is updated after each time step.}$$

The free shrinkage of wood parallel to grain is assumed to be dependent on the strain of wood, as in eq.(14). Wood then shrinks and swells more in a state of compression strain and less in a state of tension strain than when not loaded. This results in the oscillation of the creep curve in bending when subjected to cyclic humidity conditions.

$$\epsilon_u = (\alpha - b \epsilon(t)) \Delta u, \quad (14)$$

where $b = 1.3 [-]$
 α : shrinkage coefficient parallel to grain
 Δu : Moisture content increment.

To account for variable loading and creep recovery the Boltzman superposition principle is applied. Mechano-sorptive effects are also known to increase the rate of recovery of deformation when unloading.

ANALYSIS RESULTS

Eq.(4) is rearranged to determine the elastic strain increment at each node:

$$\Delta \epsilon_{E,i} = \Delta \epsilon_i - \Delta \epsilon_{visk,i} - \Delta \epsilon_{ms,i} - \Delta \epsilon_{u,i} \quad (15)$$

Using eq.(3) and eq.(6) the stress increment at each node during the current time step can be derived from:

$$\Delta \sigma_i = \{ \Delta(\partial v / \partial z) - y_i \Delta(\partial^2 \omega / \partial z^2) - \Delta \epsilon_{visk,i} - \Delta \epsilon_{ms,i} - \Delta \epsilon_{u,i} - \Delta J_{0,i} \sigma_i \} E(u_i) \quad (16)$$

The strain distribution increments are computed iteratively:

Increment of axial strain:

$$\Delta v / dz = \{ N - \sum_i (\sigma_i + \Delta \sigma_i) a_i \} / \{ \sum_i a_i E_i(u) \} \quad (17)$$

Increment of curvature:

$$\Delta d^2 \omega / dz^2 = \{ M - \sum_i (\sigma_i + \Delta \sigma_i) (y_i - y_0) a_i \} / \{ \sum_i (y_i - y_0)^2 a_i E_i(u) \} \quad (18)$$

Until the section forces are in equilibrium with the external loads:

$$\sum_i (\sigma_i + \Delta\sigma_i) a_i = N \quad (19)$$

$$\sum_i (\sigma_i + \Delta\sigma_i) (y_i - y_0) a_i = -M \quad (20)$$

The force criteria for the convergence of the iterations was chosen. This is based on the equilibrium of the internal stresses to the external loads, as in eq.(19) and eq.(20). The convergence is fulfilled when the following inequalities hold:

$$| \{ \sum_i (\sigma_i + \Delta\sigma_i) a_i - N \} / N | \leq 10^{-5} \quad (21)$$

$$| \{ \sum_i (\sigma_i + \Delta\sigma_i) (y_i - y_0) a_i + M \} / M | \leq 10^{-5} \quad (22)$$

When the equilibrium of forces convergence, the new strain values and the deflection of a beam loaded with a constant moment are:

$$\varepsilon^{t+\Delta t}(x,y) = \varepsilon^t(x,y) + \Delta\partial v / \partial z - y \Delta(\partial^2 \omega / \partial z^2) \quad (23)$$

$$w^{t+\Delta t} = w^t + \Delta(\partial^2 \omega / \partial z^2) L^2 / 8 \quad (24)$$

Where: v is displacement in z (grain) direction
 ω is displacement in y direction (height direction)

The value of the time step is chosen in a way that the stability of the computations is ensured. The computations performed to each node of the cross section follows the algorithm below:

1. Compute the moisture content distribution over the cross section.
2. Update material properties according to moisture content distribution.
3. Compute stress distribution.
 - Initially ($t=0$) according to elastic theory.
 - First iteration values from previous time step.
4. Compute strain increment at the nodes during the elapsed time step using current stress distribution and moisture content increment.

5. Calculate stress increment at each node during the elapsed time step. Return to 3 and re-estimate the strain increments, until stress and strain are in agreement.

6. Compute section forces using the stress distribution and compare if they match with the external loads N , M . If precision or convergence requirements are not satisfied return to 3. and adjust the strain distribution according to the difference of the internal and external loads considering current stiffness of the cross section.

7. Program output for current time:

- Strain distribution $\epsilon(x,y)$
- Deflection from the curvature of a beam
- Stress distribution from given sections $\sigma(x,y)$.

8. Proceed to next time step adding a time increment and return to 1.

The output from the analysis consists of moisture content, $u(x,y)$, strain, $\epsilon(x,y)$, and stress, $\sigma(x,y)$, distributions over the cross section at every time step. The strain and stress distributions are directed parallel to grain or normal to the cross section plane. The curvature values derived from the strain distributions are used to compute the creep of a beam loaded with a constant moment over a defined span.

STUDIED CASES

The analysis is used here to model the creep of timber beams, which are subjected to an outdoor relative humidity environment and to different loadings using several snow load - permanent load ratios. The bending creep of two different size beams are studied: a cross section of $50 \times 200 \text{ mm}^2$ (solid timber) and a cross section of $140 \times 900 \text{ mm}^2$ (glulam). The number of nodes used in the analysis to represent the cross sections were 9×13 and 17×39 nodes respectively.

Relative Humidity input

The relative humidity of the environment was taken from a database of the monthly mean relative humidity values outdoors for the five year period 1963 - 1967 in the Helsinki area, Finland. During this period the relative humidity varied between the extreme values of RH 55 % and RH 92 %, fig 1. Very similar

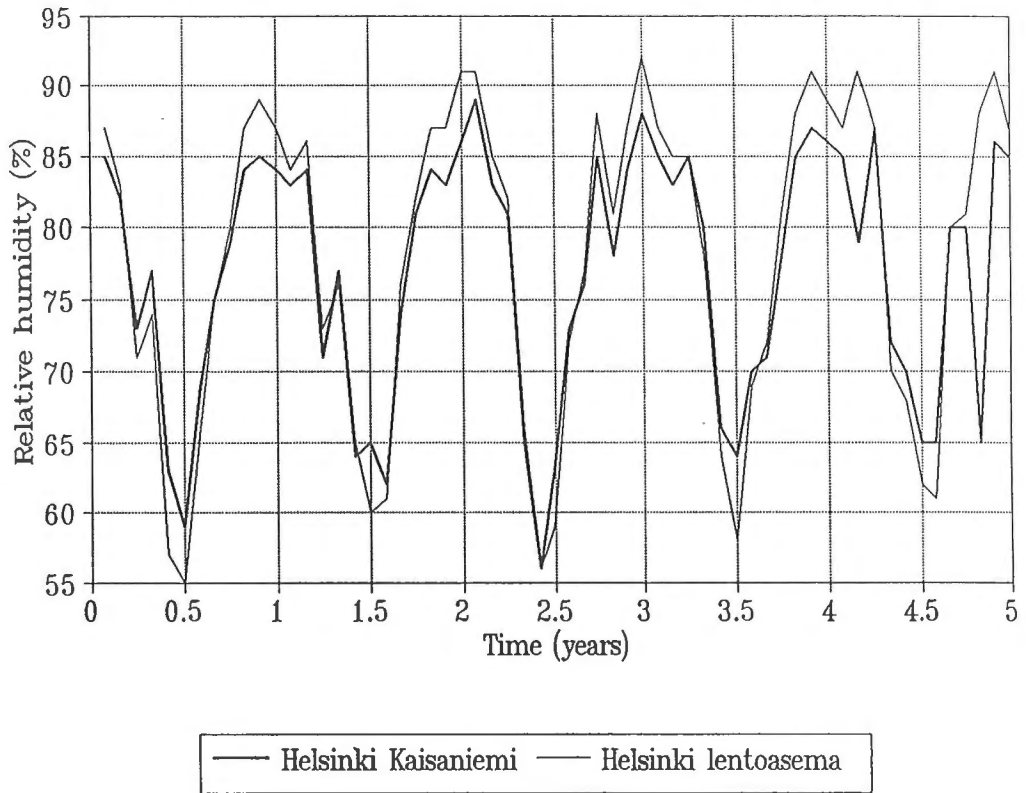


Fig. 1 Monthly mean air relative humidity from two weather stations during the years 1963 - 1967. The values registered from the airport weather station (lentoasema) were used as input to the analysis.

yearly variability of the outdoor relative humidity has been reported by Tsoumis (1964) for different locations in northern and central Europe. The humidity conditions in inhabited (heated) buildings cycle in an opposite phase, but the amplitude of the cycling is quite close to that of the outdoor air, (Thelandersson 1990). The relative humidity input used may thus represent the conditions in many locations.

The creep was computed for a period of ten years and for a period of 50 years using this relative humidity data of five years consecutively over the studied period.

Load input

The loads used in the analysis consist of a dead load and a snow load. Four different snow load - dead load ratios were considered, these were load case A: 80% - 20 %, load case B: 50% - 50%, load case C: 20% - 80% and load case D: 0% - 100% respectively.

The duration of the dead load is considered permanent. The duration of the snow load is expressed by the excursion time of the ground snow depth. The excursion time $\{\eta$ [years per year]] is the time when the magnitude of snow depth (snow load) is above a certain level. The excursion time does not give the true snow depth variation during the year, but defines the total time during the year that the snow load is above a certain level. In Forsler & al. (1975) excursion times of different snow depths in different parts of Sweden were reported. It is observed that the excursion time curve is slightly concave extending from the maximum snow depth value to a zero value. This curve can be quite satisfactorily defined by a straight line being on the safe side. The slope of this imaginary line was observed to have a constant slope of about 2 [m/(years per year)] regardless of the geographical position or ultimate snow depth.

The snow load in the analysis was thus taken as a yearly symmetric triangular load having a constant slope of 1 [m/(years per year)] regardless of the maximum load value. In all the studied cases, the maximum load is assumed to correspond a bending stress of 10 MPa. The magnitude of the maximum load (and the corresponding bending stress) specifies the relative creep value. The elastic deflection of the beam when subjected to the maximum load is defined

as a relative creep value of one and the computed creep is related to this deflection value. It is thus assumed that the beam is designed to this maximum load and the creep factors should then be relative to this calculated elastic deflection.

According to ISO CW 4355 the characteristic snow design load should be taken as the load value with a return period of 50 years. However, in modelling the creep of wood it is highly improbable that the maximum snow load is at this magnitude every year. The maximum snow load is random by nature and should be thus treated by a probabilistic basis. For this reason a simulation was carried out on the snow load portion of the total load.

Table 1. Five year and ten year return period snow depth values relative to the 50 year return period value. Ref: Forsler & al., 1975 (Snow depths, observations of 40 to 84 years) ; Katajisto, 1966 (water-equivalents, Observations of 30 to 37 years).

Location of observation	Relative values between return periods of:	
	50 year/ 5 year	50 year/ 10 year
Sweden:		
Lund	1.87	1.43
Linköping	1.74	1.43
Falun	1.61	1.36
Umeå	1.50	1.27
Östersund	1.64	1.38
Jokkmokk	1.53	1.33
Finland:		
Helsinki	1.59	1.35
Lohtaja	1.72	1.41
Pielisjärvi	1.45	1.27

Observations of the ground snow depth in Sweden (Forsler & al., 1975) and in Finland (Katajisto, 1966). The ultimate snow depth relative to the 50 year return period value is of interest. Table 1 summarizes the ultimate snow depth values

as relations of the 50 year/ 10 year and the 50 year/ 5 year return period values.

The relative snow depth values above can be classified into maritime climates of lower average snow depths having higher relative values and to continental climates of higher snow depths having lower relative values. Otherwise these values are fairly close to each other. The simulation was carried out using the snow depth values of Umeå because of the large database of this location extending over 84 years, (Actions on structures, Snow loads CIB W81). The snow depth values for the modelled 10 years and 50 years were randomly chosen from the cumulative Gamma distribution function. The snow load values of a ten year simulation is presented in fig. 3 as relative values to the characteristic value with a return period of 50 years. A separate simulation of snow depths over 50 years is presented in fig.4.

Two separate sets of computations were carried out to model 10 year creep with the described snow load - permanent load ratios. One set using the maximum snow load value of the 50 year return period for every year and one set using the simulated maximum snow loads for the ten years (fig 3.) as described above. The duration of the load is taken as described in fig. 2., load cases A,B,C and D.

The 50 year creep was modelled with the simulated snow loads using a load cases A and B as well as a load case with only the simulated snow loads (without a permanent load component) and a load case with only a permanent load (load case D, no snow load component).

COMPUTED RESULTS

The computed results in the following are presented as relative creep values, which is the creep divided by the elastic deflection when the maximum load, corresponding to a bending stress of 10 MPa, is applied.

Ten year creep: case of only a permanent load

The ten year loading (long term load) resulted in relative creep values of about 2.7 for the timber beam and 2.5 for the glulam beam when only the maximum

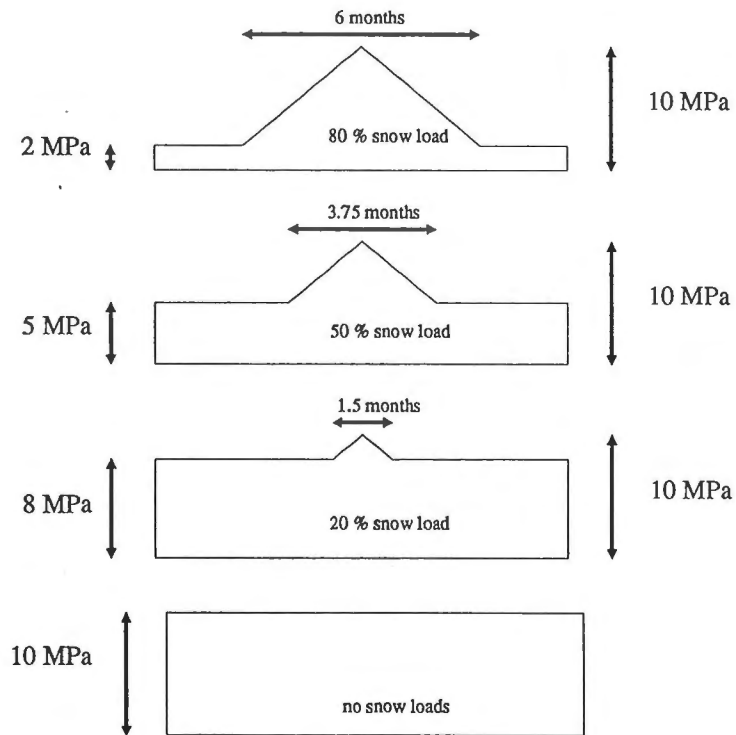


Fig.2 Four different loading cases used in the analysis. From top to bottom load cases A, B, C and D.

Simulated snow loads load relative to 50 year return period

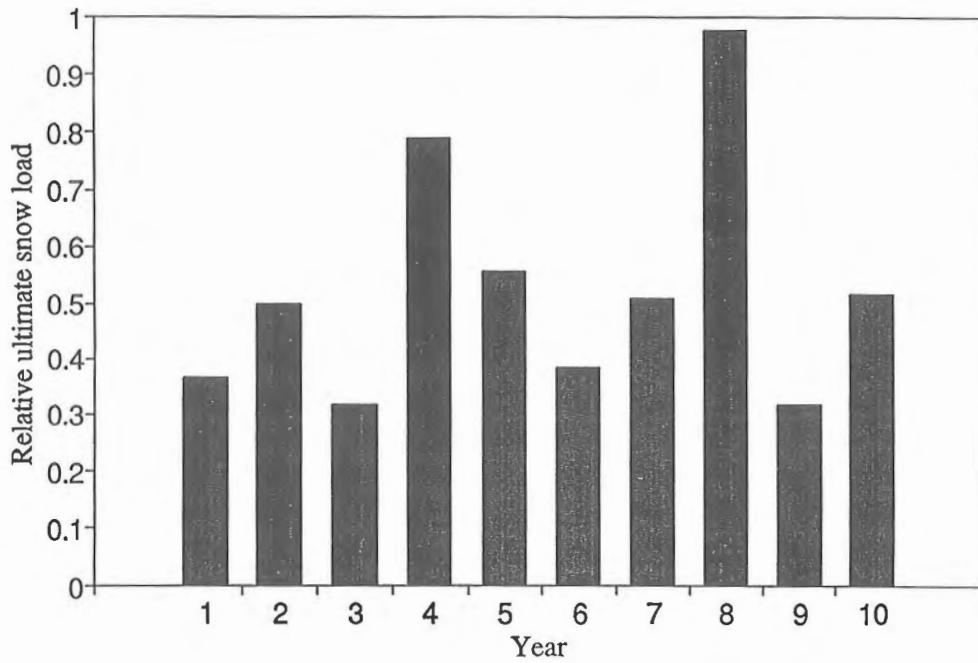


Fig.3 Simulated yearly maximum snow load values for a 10 year period relative to the 50 year return period snow load value.

Simulated snow loads load relative to 50 year return period

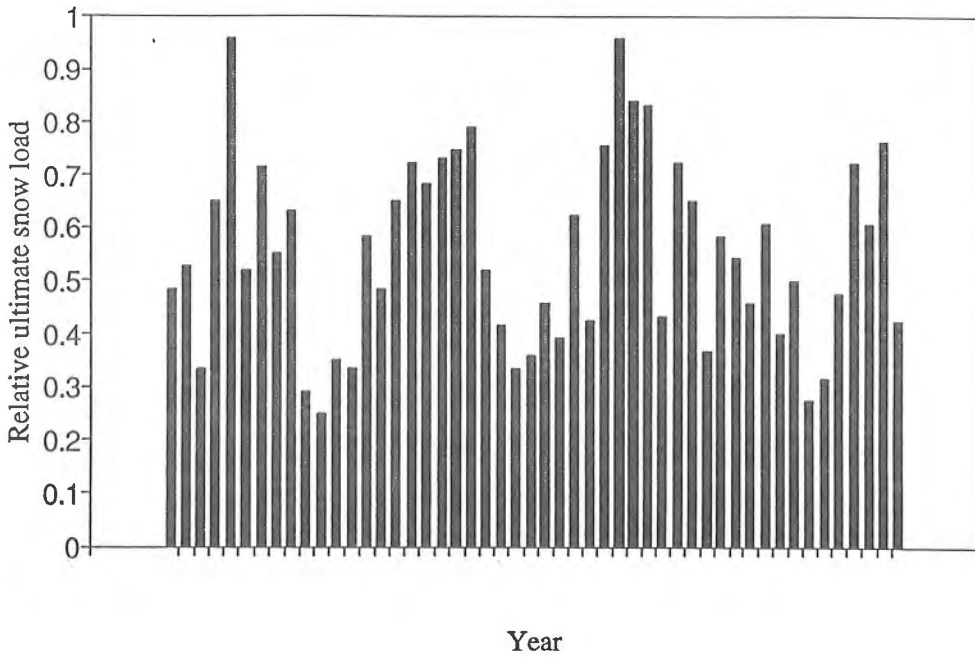


Fig.4 Simulated yearly maximum snow load values for a 50 year period relative to the 50 year return period snow load value.

constant load is applied. The relative creep at six months of loading (medium term load) was about 1.5 for the timber beam and about 1.25 for the glulam beam.

Ten year creep: case of using the 50 year return period snow load value

The existence of the snow loads considerably decreases the magnitude of creep. This is so because the reference deflection to which the creep is related is the deflection value when maximum load is applied and in the case of snow loads this maximum load is present only for a short period of time once a year. The ratio of snow load - dead load did not effect very much the ultimate creep values.

When snow loads are taken as the 50 year return period value for every year the relative creep value at an instant when the maximum load is present after ten years of loading was between 2.0 - 2.2 for the glulam beam and about 2.3 for the timber beam, fig.5 and fig.6. When the snow load is not present these relative deformation values are much lower depending on the magnitude of the permanent load. These creep values can be considered as the upper limit values, since it is unlikely that the snow load is at this magnitude annually for ten consecutive years.

Ten year creep: case of using the simulated snow load values

When the simulated snow load values are used, which were considerably lower than the 50 year return period value, the computed creep is lower than in the above case. This difference is higher the higher the snow load portion of the total load, although the ratio of snow load to permanent load did not have a very significant effect on the ultimate relative creep value during the studied ten year period.

For load cases A and B (snow loads 80% and 50 % of total load) the relative creep reaches a maximum value of about 2.0 for the timber beam and about 1.7 for the glulam beam. This value occurred during the eighth year when the snow load was quite close to the 50 year period return value.

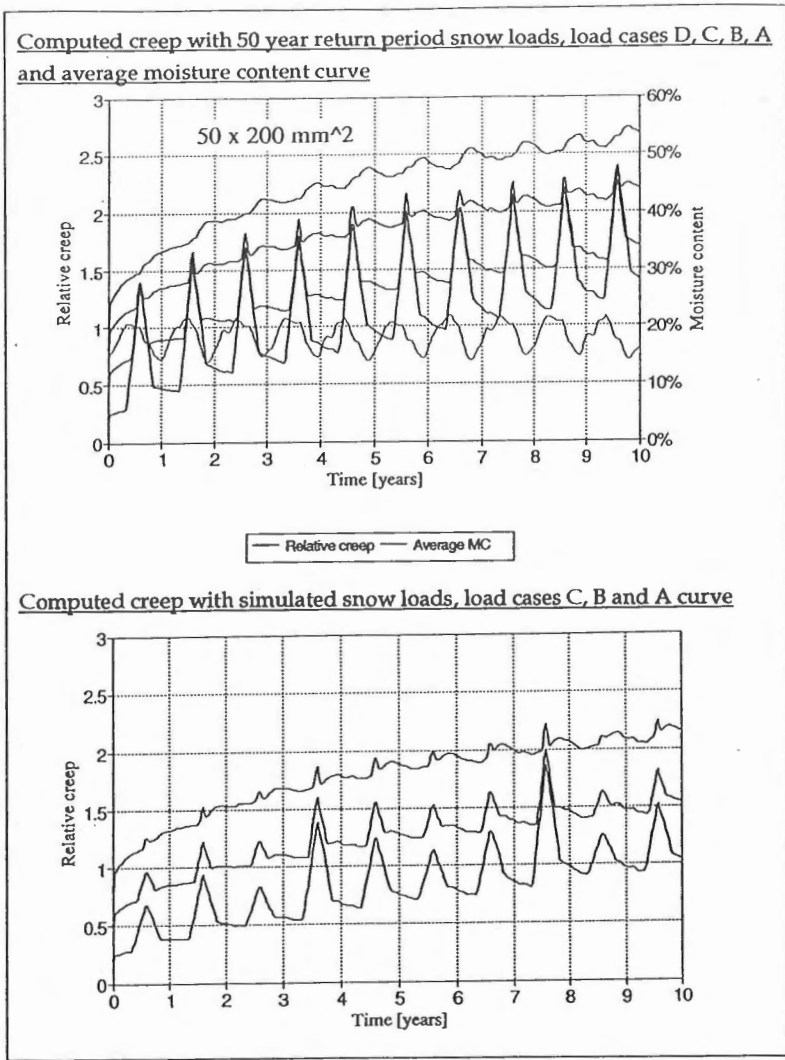


Fig.5 Computed creep for 10 years of the 50 x 200 mm² beam using the four different loading cases (snow load - permanent load ratios). Above: using the 50 year return period snow load value as the maximum snow load value for every year. Below: using the simulated maximum snow load values (as in fig.3).

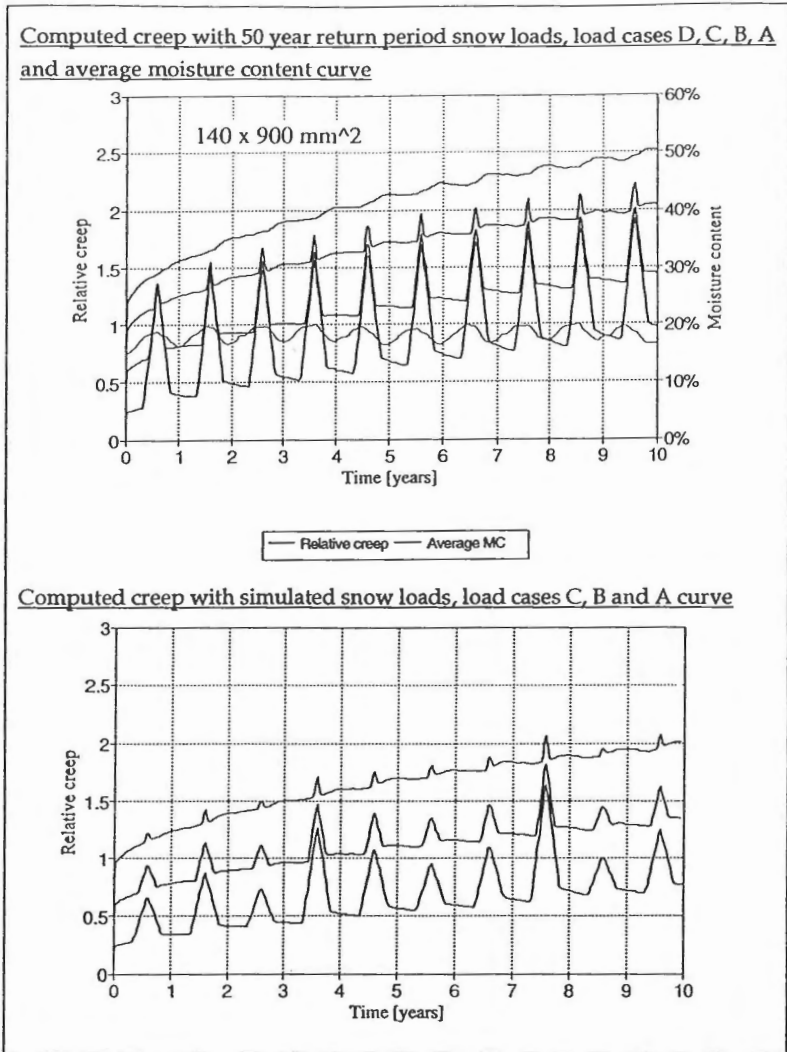


Fig.6 Computed creep for 10 years of the 140 x 900 mm² beam using the four different loading cases (snow load - permanent load ratios). Above: using the 50 year return period snow load value as the maximum snow load value for every year. Below: using the simulated maximum snow load values (as in fig.3).

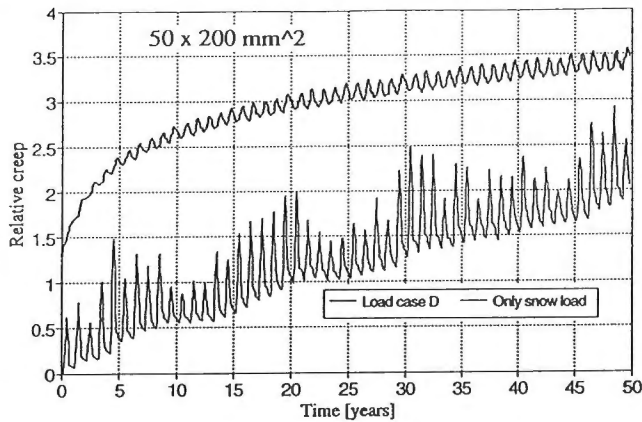
Fifty year creep

The results of the 50 year creep are given in fig.7 for the timber beam and fig.8 for the glulam beam. In case of only a permanent load (load case D) there is not very much difference on the computed creep for the timber and the glulam beams, but in the load case of only snow loads the smaller size timber beam resulted in higher creep. This can also be seen from the results of load cases A and B, where the creep of timber beam seems to be independent of the snow load ratio. For the glulam beam there is difference in creep between load cases A and B.

DISCUSSION

According to the Eurocode draft 5 'if a load combination consists of actions belonging to different load-duration classes the deflection should be calculated separately for the different actions with the appropriate creep factors'. In the computations carried out snow loads and permanent loads were considered. These are classified according to their duration to medium term and permanent actions respectively. From the computed results where the load cases of a permanent load and a snow load were considered separately, deformation factors presented in table 2 were derived. These factors give about the same creep values when compared to the other load cases considered where both permanent and snow loads were present.

Computed creep for 50 years loading, load case of only a permanent load and a load case of only the simulated snow loads



Computed creep for 50 years loading with the simulated snow loads, load cases B and A curve

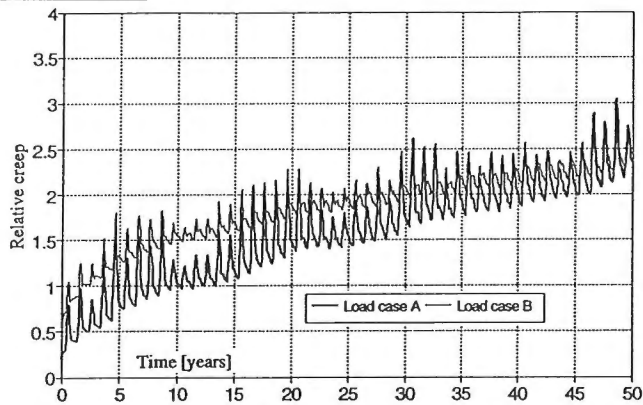
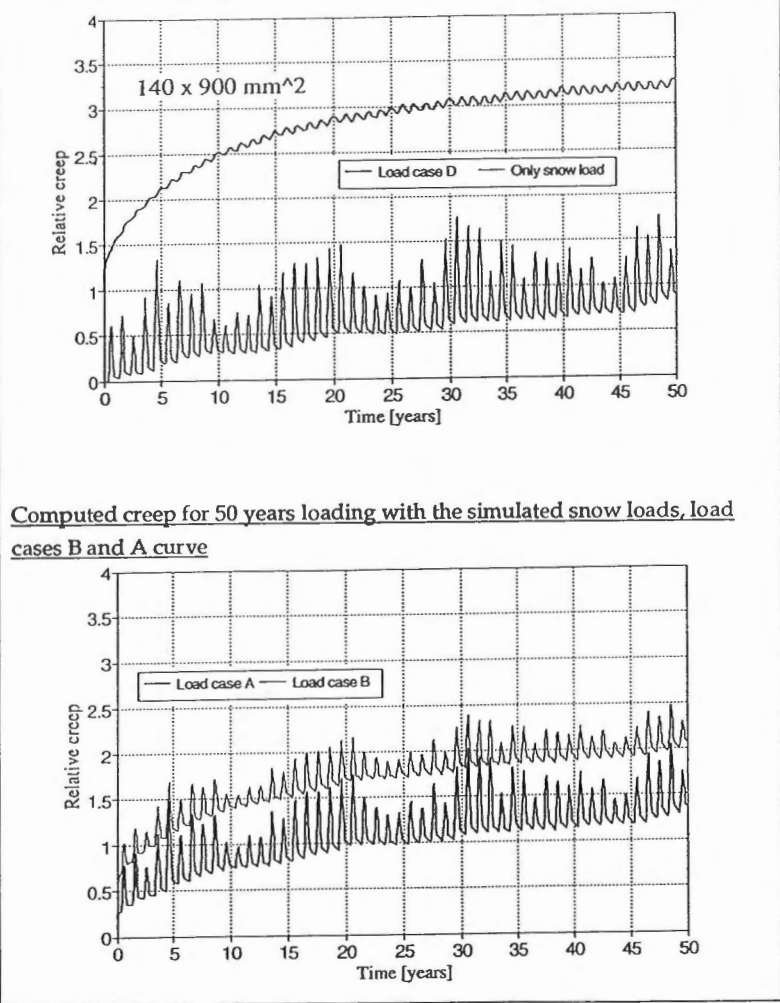


Fig.7 Computed creep for 50 years of the $50 \times 200 \text{ mm}^2$ beam using several loading cases (snow load - permanent load ratios). Above: using only a permanent load and only a simulated maximum snow load. Below: using load cases A (80% snow load) and B (50% snow load) with simulated maximum snow load values (as in fig.4).

Computed creep for 50 years loading, load case of only a permanent load and a load case of only the simulated snow loads



Computed creep for 50 years loading with the simulated snow loads, load cases B and A curve

Fig.8 Computed creep for 50 years of the 140 x 900 mm² beam using several loading cases (snow load - permanent load ratios). Above: using only a permanent load and only a simulated snow load. Below: using load cases A (80% snow load) and B (50% snow load) with simulated maximum snow load values (as in fig.4).

Table 2. The values of k_{def} for solid timber and glulam. Derived from fig. 7 and 8 where the load cases of a permanent load and a snow load were considered separately. {Relative creep : $1 + k_{def}$ }

	10 year creep	50 year creep
Timber:		
Medium term load	0.5	1.9
Permanent load	1.7	2.5
Glulam:		
Medium term load	0.4	0.8
Permanent load	1.5	2.2

Summary of main assumptions of the model

The definition of solid timber and glulam is here only specified by the member size. The chosen sizes were assumed to represent the respective material. The material properties were assumed to be the same.

The relative humidity input was given as the monthly average value. It is assumed that humidity cycles of shorter wave length does not significantly effect the moisture content of the member. The validity of this assumption is governed by the surface emissivity value of moisture transfer, which is a parameter not well known.

In the simulation of the snow load, only the yearly maximum snow load value was simulated. The duration of the load is relative to this load value and was assumed symmetric and triangular.

It is assumed that the material models as well as the material parameters are valid up to the studied structure lifetime of 50 years. It is possible that these models or respective parameters change as a result of ageing of the wood, but since such knowledge is not available, it is relied on the behaviour observed from test results.

There are some unsolved questions regarding the creep of wood which might also alter the model presented here. One of these is the effect of temperature and changes of temperature on creep. The experiments, from which the model was derived, were carried out in constant room temperature and the model used in the analysis does not account for changes in temperature. The modelling of moisture transfer in wood in natural humidity conditions is not well known. Diffusion and surface emissivity coefficient values given in literature are well scattered from source to source and their dependencies on temperature, air velocity or on the aging of wood is not known.

REFERENCES

- Anon. 1990: Eurocode 5 Design of Timber Structures. Working draft, October 1990.
- Anon. 1991: Actions on structures, Snow loads. CIB commission W81. First edition.
- Anon. 1991: ISO CW 4355 Bases for design of structures - Determinations of snow loads on roof structures.
- Forsler S, Jonasson H., Landin W., Schärnell L., Åkerlund S. 1971: Snödjup och vattenvärde. (In Swedish) Rapport 24, Institutionen för Byggnadsteknik, Lund Institute of Technology, Lund Sweden.
- Hunt D.G., Shelton C.F. 1988: Longitudinal moisture-shrinkage coefficients of softwood at the mechano-sorptive creep limit. *Wood Sci. Technol.* 22:199-210.
- Katajisto R. 1966: Tutkimus kattorakenteita rasittavista lumikuormista. Diplomityö. (In Finnish). Helsinki University of Technology, Finland. 61 p.
- Mendelson A.; Hirschberg M.H.; Manson S.S. 1959: A general approach to the practical solution of creep problems. *J. Basic. Eng. Trans. ASME* 81 ser D (1959) 585-598.
- Mohager S. 1987: Studier av krypning hos trä (Studies of creep of wood, in Swedish). Doctoral dissertation. Kungliga Tekniska Högskolan, Stockholm Sweden. 139 p.
- Mohager S., Toratti T. 1992: Long term bending creep of wood in cyclic relative humidity. To be published in *wood Sci. Technol.*

Patankar S.V. 1980: Numerical heat transfer and fluid flow. Hemisphere publishing corp. Washington, New York, London. 167 p.

Thelandersson S. 1987: Notes on linear viscoelasticity. Report TVSM-3009, Lund Institute of Technology, Division of Structural Mechanics, Lund Sweden.

Thelandersson S. 1990: Variation of moisture content in timber structures. IUFRO 5.02 St. John Canada.

Toratti T. 1991a: Creep of wood in varying environment humidity, Part I Simulation of creep. Report 19. Laboratory of Structural Engineering and Building Physics. Helsinki University of Technology. Finland.

Toratti T. 1991b: Long term bending creep of wood. Proc. CIB-W18 Oxford UK.

Tsoumis G. 1964: Estimated moisture content of airdry wood exposed to the atmosphere under shelter, especially in Europe. Holzforshcung 18.

Tomi Toratti, Lic. Tech., Research engineer
Laboratory of Structural Engineering and Building Physics
Civil Engineering Department
Helsinki University of Technology